

Quantitative analysis of total magnetic anomaly maps on archaeological sites—Part 1

Hazel Deniz Toktay^{ID} | Davut Aydoğan^{ID} | Fethi Ahmet Yüksel^{ID}

Geophysical Engineering Department,
Istanbul University- Cerrahpasa, Istanbul,
Turkey

Correspondence

Hazel Deniz Toktay, Geophysical
Engineering Department, Istanbul
University- Cerrahpasa, Istanbul, Turkey.
Email: hazel.deniztoktay@iuc.edu.tr

Communicated by: M. Efendiev

In this study, which is the first part of quantitative analysis of total magnetic anomaly maps on archaeological sites, it is aimed to analyze the horizontal boundary values of potential buried structures that cause anomalies from the total magnetic anomaly maps of an archaeological excavation area. In the first step, the model was created in accordance with the archaeological structure. Noisy and noiseless anomaly maps of this model were calculated. These maps were enhanced using the reduction to pole and upward continuation methods. Tilt angle and automatic gain control methods were used. The responses of these methods on the total magnetic anomaly maps of the model were analyzed. In the second step, by applying the same procedures on the total magnetic anomaly map obtained from the magnetic measurements on the area that has not been excavated in the Amasya Oluz Mound archaeological excavation area, the horizontal boundaries of the potential structure elements of the region were analyzed.

KEYWORDS

automatic gain control, geophysics, quantitative analysis, tilt angle, total magnetic anomaly map

MSC CLASSIFICATION

86A04; 86A20

1 | INTRODUCTION

Nondestructive geophysical methods have a significant role in archaeological prospection. The use of measurements obtained from geophysical methods rather than direct excavations is a more reliable and preferred way of preserving the historical heritage in archaeological studies planned to be carried out in large areas. It is possible to image the subsurface from a different perspective and project archaeological surveys using archaeogeophysical methods. The magnetic method is frequently used for rapid and successful exploration of large areas. Basic structures such as entrances, roads, monuments, and covered walls, which constitute the building blocks of historical settlement areas, can be determined by measuring the magnetic sensitivity values.¹ In the archaeological surveys, magnetic measurement data, which is one of the geophysical exploration methods, can be interpreted to find the remains of temples, graves, walls, foundations, and similar historical remains buried subsurface.

Abbreviations: AGC, automatic gain control; RTP, reduction to pole; TA, tilt angle.

During the magnetic data interpretation process, determining approximate horizontal boundaries of the features causing anomalies is essential to obtain maximum information from the total magnetic anomaly maps. In determining the boundaries of potential structures, edge detection methods are known as the most preferred classical methods. Many derivative-based algorithms such as horizontal gradient magnitude, analytical signal, theta map, tilt angle (TA), and analytical signal methods have been developed to analyze the horizontal locations of potential subsurface structures, which may cause anomalies. The first research to determine the edges of geological features is the vertical derivative method proposed by Evjen.² Miller and Singh³ have developed the TA method and compared this method to horizontal derivative, second vertical derivative, and analytical signal techniques. Wijns et al⁴ have developed the theta map algorithm to apply edge detection methods. Cooper and Cowan⁵ have tested the TA method to detect edges of features causing anomalies by making further developments of the synthetic model and field data applications. The TA method presented by Miller and Singh³ is rearranged by Salem et al.⁶ Verduzco et al⁷ and Ma and Li⁸ have confirmed by their surveys that the maximum value of the total horizontal derivative can highlight the edges of potential structures more accurately.

In this study, quantitative analyses were performed using derivative-based methods to detect the horizontal locations of potential subsurface structures that cause anomalies on total magnetic anomaly maps. In the first stage, to test the compatibility of these methods with actual field data, a synthetic model was created compatible with the archaeological structures. The total magnetic anomaly maps obtained from the noisy and noiseless data belonging to this model were prepared to analyze the structures. These maps are enhanced by applying reduction to pole (RTP) and upward continuation processes to eliminate the interfering factors such as noise and inclination angle. The horizontal locations of the blocks were determined by applying the TA and automatic gain control (AGC) methods. In the second stage, similar quantitative analyses have been made on the total magnetic anomaly map of actual field data, and the locations of potential structures are determined.

2 | DATA ENHANCEMENTS

The presence of interfering factors such as geological noise, physical noise, multiple sources, or errors in data acquisition can cause complications during the magnetic data analysis. This type of adverse complications will cause potential building elements in the study areas to be located in different locations than they should be. Therefore, these negative effects should be eliminated from the total magnetic anomaly maps. These maps should be enhanced before performing quantitative analysis of locations.

2.1 | Upward continuation method

The upward continuation method provides the result as if the potential field data measured on a surface were measured on a surface higher than the sources. This transformation tends to attenuate anomalies depending on the wavelength. Attenuation is realized inversely proportional to the wavelength. The upward analytical continuation process reduces the measured data. In some cases, it may be necessary to compare or combine data measured at significantly different heights. In such cases, this method enables transforming data as measured on a particular surface. The upward continuation method highlights the anomalies caused by deep sources. For example, in a magnetic survey conducted on a terrain dominated by young volcanic units, short-wavelength anomalies may prevail due to near-surface volcanic rocks in the data. In this case, the anomalies caused by shallow sources can be suppressed by applying the upward continuation method to the data to clarify the anomalies caused by the plutonic rocks located in deeper.⁹

If the U function is a harmonic, continuous function and has continuous derivatives along a regular R region, the U value in each P point in the R region (Figure 1) from Green's third equation

$$U(P) = \frac{1}{4\pi} \int_S \left(\frac{1}{r} \frac{\partial U}{\partial n} - U \frac{\partial}{\partial n} \frac{1}{r} \right) dS \quad (1)$$

can be obtained. In this relation, which is the basic principle of the upward continuation method, S denotes the boundary of the R region. Here, n is the normal outward direction, and r denotes the distance from P to integration over region S . The potential field can be calculated at every point according to the behavior of a region on a certain surface.⁹

The most basic analytical extension for the potential field is that the calculation is done on a flat surface. Here, classical derivative methods defined by Henderson and Zietz¹⁰ were used. Using the Cartesian coordinate system where the z axis is downward, it is assumed that the potential field is calculated on a flat surface (at $z = z_0$) and derived from a single point

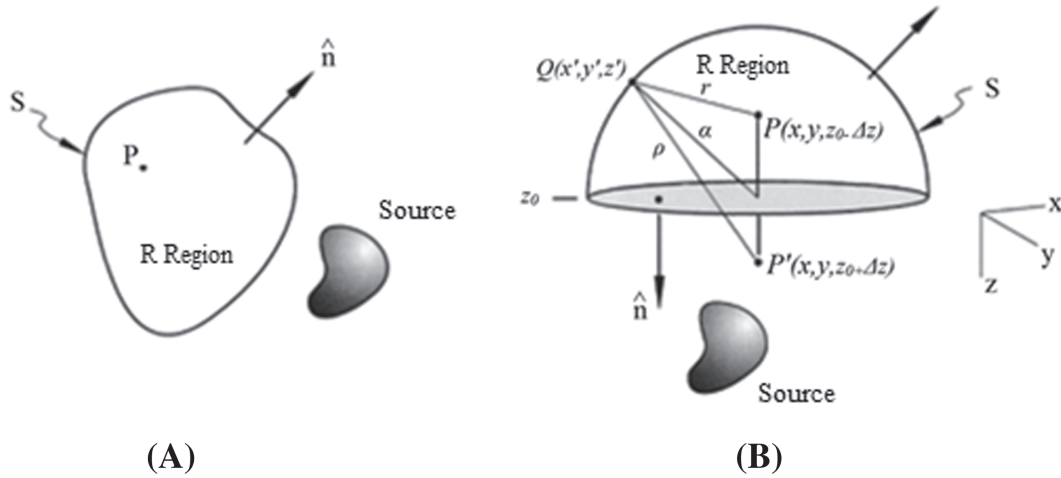


FIGURE 1 (A) Harmonic function in the R region can be evaluated at any point in R according to its behavior at the S boundary. The unit vector perpendicular to the surface S is denoted by n ; (B) shows the upward analytical extension from horizontal surfaces. The potential field is $z = z_0$ on the horizontal surface, and it is required to be at the point $P(x, y, z_0 - \Delta z)$ ($z > 0$). Surface S consists of a hemispherical plane of radius α in addition to the horizontal surface. The P' point is a mirror image of the P point projected onto the surface. The integration point Q is on the surface S . r and ρ indicate the distance from Q to P and Q to P' , respectively⁹

$P(x, y, z_0 - \Delta z)$ where its value on the surface is greater than 0. The S surface consists of a flat surface and a hemisphere of radius α (Figure 1).

Considering that all surfaces are located in the region where $z > z_0$, as seen in Equation (1), the integration of the equation on the hemisphere gets smaller as the angle α increases. Consequently, if $\alpha \rightarrow \infty$,

$$U(x, y, z_0 - \Delta z) = \frac{1}{4\pi} \int_{-\infty}^{\infty} \int_{-\infty}^{\infty} \left(\frac{1}{r} \frac{\partial U(x', y', z_0)}{\partial z'} - U(x', y', z_0) \frac{\partial}{\partial z'} \frac{1}{r} \right) dx' dy' \quad (2)$$

the equation is obtained and the value of r in this relation is

$$r = \sqrt{(x - x')^2 + (y - y')^2 + (z_0 - \Delta z - z')^2} \quad (3)$$

and it is expressed as $\Delta z > 0$.

In Equation (2), it is necessary to know not only the value on the U surface but also the vertical gradient value. This situation is not suitable for many practical applications. For this reason, Green's second equation is added to Equation (1) in order to eliminate the derivative term in Equation (2). Here, the equation is reached by using Green's second equation,

$$\frac{1}{4\pi} \int_S \left(V \frac{\partial U}{\partial n} - U \frac{\partial V}{\partial n} \right) dS = 0 \quad (4)$$

where the V function is a harmonic function along the R region.

$$U(P) = \frac{1}{4\pi} \int_S \left[\left(V + \frac{1}{r} \right) \frac{\partial U}{\partial n} - U \frac{\partial}{\partial n} \left(V + \frac{1}{r} \right) \right] dS \quad (5)$$

In order to simplify the first term of the integral, the harmonic V function must satisfy the condition $V + 1/r = 0$ at each point on the S surface. The P' point, which is the symmetry of the P point, is created in the $(x, y, z_0 + \Delta z)$ region, and

the equation below is obtained by providing the $V = -1/\rho$ condition.

$$\rho = \sqrt{(x - x')^2 + (y - y')^2 + (z_0 + \Delta z - z')^2} \quad (6)$$

While defining the V function, the expression $V + 1/r = 0$ exists on the horizontal surface. But this expression will disappear on the hemisphere as the angle α gets larger. However, the V function is always harmonic, and the value of r never disappears. After making the necessary arrangements in the above equations, the expression in Equation (2) takes the form of the following.

$$U(P) = \frac{1}{4\pi} \int_{\infty} \left[\left(\frac{1}{r} - \frac{1}{\rho} \right) \frac{\partial U}{\partial n} - U \frac{\partial}{\partial n} \left(\frac{1}{r} - \frac{1}{\rho} \right) \right] dS \quad (7)$$

Here, the expression obtained when z is moved on the horizontal surface, and the derivative is realized and is defined as the upward analytical extension integral (Equation 8). This integral gives how to calculate the potential field at any point above a certain level.⁹

$$U(x, y, z_0 - \Delta z) = \frac{\Delta z}{2\pi} \int_{-\infty}^{\infty} \int_{-\infty}^{\infty} \left(\frac{U(x', y', z_0)}{[(x - x')^2 + (y - y')^2 + \Delta z^2]^{3/2}} \right) dx' dy' , \Delta z > 0 \quad (8)$$

The amplitude of the magnetic field over the effective mass varies as an exponential function of the wavelength with height. The effect of this relationship can be easily eliminated by remeasuring the area at the highest height (upward continuation) or at the lowest (downward continuation) with the fast Fourier transform (FFT).¹¹

2.2 | Reduction to pole method

RTP is a standard part of magnetic data processing, especially in large-scale magnetic anomaly maps. This process converts the magnetic anomaly caused by a source into an anomaly located at the pole of the same source and produced as if it were only in an induction magnetized environment. It also helps in the interpretation of magnetic data in later stages by eliminating the magnetic latitude effect. In the pole reduction process, magnetic data collected at different latitudes are generally simplified. Unless both the magnetization and the geomagnetic field are vertically oriented, the magnetic anomaly cannot be viewed directly above the impact mass. This method converts the magnetic field at the magnetic latitude where the earth's field is tilted to the field at the magnetic pole where the induced field is vertical.¹² When the earth's field is inclined, magnetic anomalies due to induction are asymmetric with respect to the source, whereas magnetic anomalies occur directly above the source if the induced field is in the vertical direction.¹³ The most prominent feature in gravity and magnetic methods is that although gravity anomalies tend to be above the mass density in gravity method, this situation differs in magnetic anomalies when both magnetization and ground magnetic field are not in vertical direction. Unless the unit vectors in the direction of magnetization (\hat{m}) and the surrounding field (\hat{f}) are vertical, the phase angles of the magnetization (θ_m) and the ground magnetic field (θ_f) cause phase changes in magnetic anomaly, such as lateral shifts, distortions, and even sign changes⁹ (Figure 2).

The RTP process works by shifting the phase (assuming that the data is collected at the magnetic pole) to eliminate the asymmetry caused by the inclination angle. Thus, by shifting the anomaly laterally, centering on the source is provided, and interpretation operations are facilitated.

Pole reduction is performed in order to eliminate the asymmetry in the anomaly. Any ΔT_r anomaly transformed in the Fourier environment can be expressed as Equation (9).

$$F[\Delta T_r] = F[\psi_r] F[\Delta T] \quad (9)$$

where the RTP $F[\psi_r]$ process can be calculated by the Equation (10).

$$F[\psi_r] = \frac{1}{\theta_m \theta_f} = \frac{|k|^2}{a_1 k_x^2 + a_2 k_y^2 + a_3 k_x k_y + i |k| (b_1 k_x + b_2 k_y)} , |k| \neq 0 \quad (10)$$

The $F[\psi_r]$ process is called RTP due to the transformation of the ΔT_r anomaly into a measurement made at the north magnetic pole where the magnetization and geomagnetic field are vertical.¹⁴

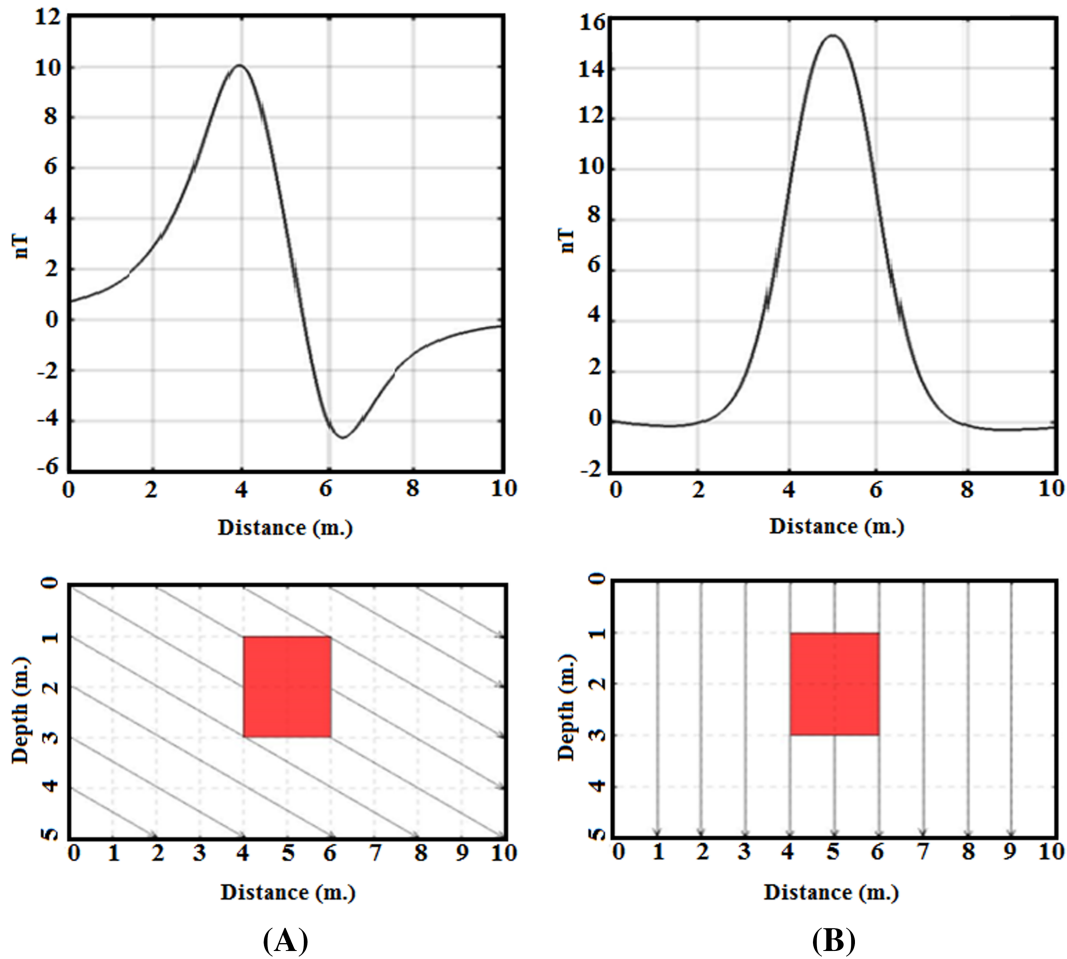


FIGURE 2 (A) The magnetic anomaly of a vertical prismatic model with an inclination angle of 45° . (B) The magnetic anomaly of the same model after the reduction to pole process [Colour figure can be viewed at wileyonlinelibrary.com]

3 | DETECTION OF HORIZONTAL BOUNDARIES

3.1 | Tilt angle method

The TA method is one of the classical derivative-based methods that detect and improve the properties of the active source edges that cause potential field anomalies. Since the magnetic anomaly amplitude depends on the magnetic field strength and magnetic source depth, low amplitude anomalies are suppressed by high amplitudes. Therefore, edge detection filters usually are applied to determine linear features without reducing long-wavelength anomalies.¹⁵ The derivative-based TA filter highlights short wavelengths in anomaly maps and reveals subsurface source boundaries that cause magnetic data.⁷ The TA derivative filter is also used in the AGC filter, which balances the responses of strong and weak anomalies. Methods that use the TA derivatives have generally been developed to quickly determine the horizontal positions and depths of the active sources that cause the anomaly.^{6,7} The TA method includes both horizontal and vertical gradients of the total magnetic field data in order to obtain the normalized derivative value based on the ratio of gradients. This method, which is one of the local phase filters, was first developed by Miller and Singh³ and is expressed by the following equation:

$$\theta = \tan^{-1} \left(\frac{\partial M / \partial z}{\partial M / \partial h} \right) \quad (11)$$

where θ is the TA and M is the total magnetic field value. The first derivative of the total magnetic field value in the horizontal direction can be denoted as follows.

$$\frac{\partial M}{\partial h} = \sqrt{(\partial M / \partial x)^2 + (\partial M / \partial y)^2} \quad (12)$$

The angle θ , which is the ratio of the vertical derivative to the absolute amplitude of the total horizontal derivative, is expressed as T in the TA method and is called the TA and be shown with the Equation (13).

$$T = \tan^{-1} \frac{\partial M / \partial z}{\sqrt{(\partial M / \partial x)^2 + (\partial M / \partial y)^2}} \quad (13)$$

In this method, the horizontal derivative values outside the active source causing the anomaly are maximum and negative. It has values in the range of TA (-90° , 90°). This feature of the method allows for an easier interpretation of the data in the evaluation phase than the analytical signal. Since the operations used in the TA method are based on the ratio of derivatives, the filter result does not contain amplitude information. Therefore, the degree of enhancement of this filter varies according to the local amplitude of the derivatives. There is no signal to improve in low gradient areas, but the output of the filter can be defined for the whole area. Therefore, the TA images must be interpreted in conjunction with the original data. TA and analytical signal approaches are methods expressed with horizontal and vertical derivatives. The approaches above tend to increase the field changes formed by shallow sources and are interrelated methods to provide information about the locations of vertical boundaries.

3.2 | Automatic gain control method

The AGC method is a data enhancement method that balances the amplitudes of anomalies by separating the dominant wavelengths. The parameters that affect this method are the size of the sliding window from which the gain is calculated and the gain function that controls the relative magnification in signal and noise. A standard gain function is considered the inverse of the square root value in the window. For varying wavelength (spatial frequency) anomalies, selecting the WS gives preliminary information about the values between which the output data is optimized. Test applications with various gain functions and WSs should be performed to obtain the most relevant result. This method can be applied to profile data as well as grid data.¹⁶

The AGC method is used to determine the regions that create significant magnetic contrast even in noisy data and to visualize faults and dike-like structures expressed in linear form. High amplitude anomalies suppress low amplitude anomalies due to the amplitude of the anomalies depending on the magnetic field strength and the depth of the source sources causing the anomalies. Rajagopalan and Milligan¹⁶ stated that in determining these types of sources, results could be obtained by focusing on increasing the relative amplitudes and the displacements of the sources.

Many methods are used to improve the image. Horizontal gradient, vertical gradient, and sunshading methods are some of the most commonly used image enhancement filters. Horizontal and vertical gradients are used to reveal the distortions and discontinuities in anomaly trends and reveal hidden sources. Especially in vertical gradient maps, short-wavelength anomalies are enhanced, while long-wavelength anomalies are attenuated. Sunshading is a directional filter that improves sources in a specific direction and suppresses sources positioned perpendicular to the desired direction.¹⁷ However, in the image processing phase, it is desired to imaging both short-wavelength and long-wavelength anomalies together. The mentioned horizontal gradient, vertical gradient, and sunshading methods are not very efficient in this context. To overcome this situation, Rajagopalan^{18a} and Rajagopalan and Milligan¹⁶ used the AGC method, which improves the amplitude of short-wavelength anomalies without eliminating long-wavelength anomalies. In this method, which can be applied to data from both profile and grid plane, AGC operation for grid data is provided by the Equation (14) as

$$A_{xy} = (Gain_{xy}) (F_{xy}) \quad (14)$$

where F_{xy} is the input function in x and y directions, $Gain_{xy}$ is the gain function, and A_{xy} is the output obtained after AGC. In order to determine the gain function, the window size (WS) must be calculated. To calculate the WS,

$$WS = \frac{1}{(2v + 1)(2w + 1)} \quad (15)$$

Block no	y axis		x axis		Depth values		Magnetic susceptibility (SI)
	Y1 (m)	Y2 (m)	X1 (m)	X2 (m)	H1 (m)	H2 (m)	
1	2	13	2	3	0.5	3.5	0.020
2	12	13	3	9	0.5	3.5	0.020
3	7	9	4	9	1.0	2.0	0.010
4	5	6	4	8	0.5	1.0	0.015
5	1	4	5	9	1.0	2.5	0.012

TABLE 1 Synthetic model parameters

expression is used. The gain function obtained by combining Equations (14) and (15) is shown in Equation (16) as

$$Gain_{xy} = \frac{1}{(2v+1)(2w+1)} \left[\sum_{i=x-v}^{i=y+v} \sum_{i=x-w}^{i=x+w} F_{ij}^p \right]^r \quad (16)$$

where the symbols v and w indicate the WS. The symbol p means the power, and the symbol r means the degree of the root. The p and r values specified in this equation are obtained by taking 2 and 0.5, respectively, to equal the inverse of the root mean square (root mean square) value. The input waveform consists of many different amplitudes. The amplitude of the input data is defined using the RMS calculation to transform the data into a constant amplitude output data. After the gain function is calculated inversely proportional to RMS, the AGC process is completed by calculating the output function depending on the WS. If the input signal has different amplitudes but one wavelength and the WS is set at the same value as the wavelength, the output signal will have a fixed amplitude value.^{16,18}

4 | SYNTHETIC MODEL APPLICATIONS

Synthetic data of potential subsurface sources were calculated to test the accuracy of these methods on field data. In the first stage, a synthetic model has been designed with the geometric parameters given in Table 1. The 3-D spatial location and the 2-D top view of the model are shown in Figure 3A,B. The model is suitable for wall and cemetery structures in archaeological sites, and it comprises five prismatic blocks with different magnetic susceptibility values. Prismatic blocks of different sizes are placed at different depths. Values of magnetic field strength and declination angle are 45 000 nT, 0°, respectively. It has been assumed that there is no remanent magnetization.

Two theoretical anomalies of the synthetic model structure given in Figure 3 were calculated using the Matlab program. The theoretical anomalies calculated by assuming the inclination angle as 60° for the first theoretical anomaly and as 90° for the second theoretical anomaly are shown in Figure 4A,B, respectively. The theoretical anomaly obtained by assuming the inclination angle 90° is designed to be used for testing purposes while RTP. In order to simulate the field measurements, Gaussian noise with a standard deviation of 0.3 nT is added to the theoretical anomaly shown in Figure 5A, and it is shown in Figure 5B.

A noisy total magnetic anomaly map, which conforms to field data, is used in analyzing. During the quantitative analysis of the theoretical data, it is necessary to eliminate the errors that may occur due to the inclination angle different from the vertical in determining the locations of the potential subsurface source distributions that cause magnetic anomalies. For this purpose, a program used to calculate RTP operations in the Matlab environment has been prepared. Noiseless data of the model have an inclination angle of 60° entered into this program, and the angle value was moved to the vertical (Figure 6A,B).

In the case of using data with noise, the negative effects of the noise and inclination angle are eliminated by applying the upward continuation and RTP processes. The upward continuation map is shown in Figure 7A after the 3-m upward continuation process is applied to the theoretical total magnetic anomaly map with noise. The RTP map is given in Figure 7B. It is observed that there is a great similarity between the RTP map of data without noise (Figure 6B) and the RTP map of data with noise (Figure 7B).

To determine the horizontal boundaries of subsurface archaeological structures using field data, the codes of the TA and AGC algorithms were written in the Matlab, and programs were prepared. The theoretical total magnetic anomaly map values were used as input data in the programs prepared to determine the horizontal boundaries of the potential subsurface features that caused the obtained theoretical data, and the results of the programs were examined. By comparing the actual locations of the subsurface model with the locations calculated from the methods used, the criteria for determining the discontinuities were tried to be examined. Therefore, the applicability of the algorithms used in

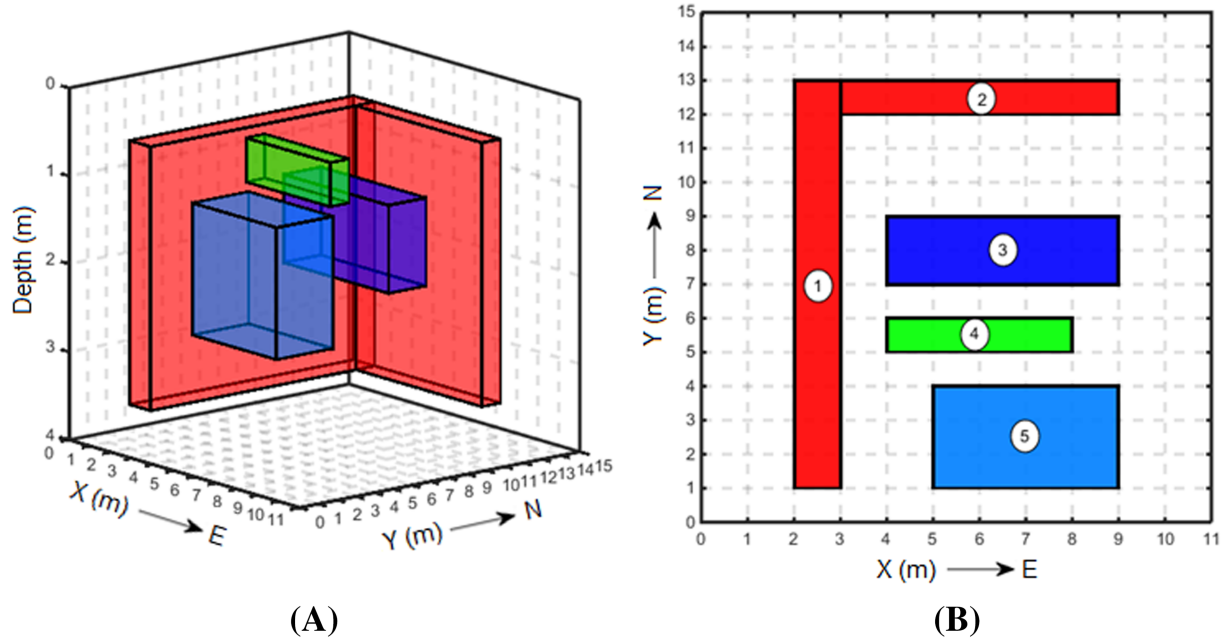


FIGURE 3 Synthetic archaeological model. (A) 3-D geometric position of the model consisting of five prismatic blocks and (B) 2-D top view of the synthetic model [Colour figure can be viewed at wileyonlinelibrary.com]

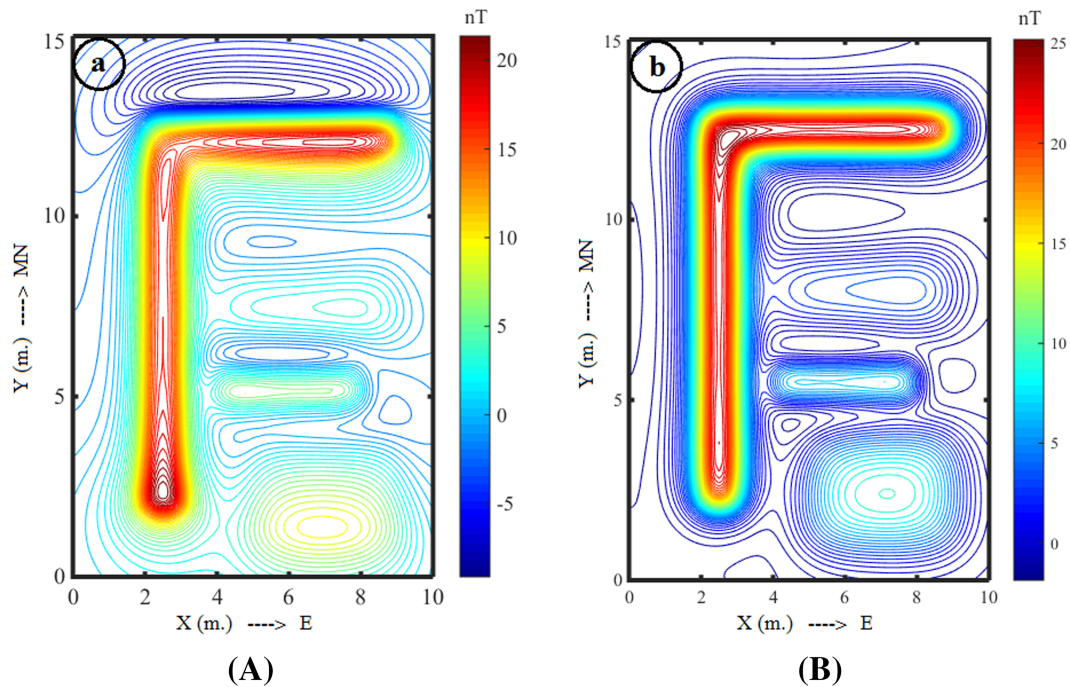


FIGURE 4 Theoretical total magnetic anomaly map of the synthetic model. (A) Inclination angle 60° and (B) inclination angle 90° [Colour figure can be viewed at wileyonlinelibrary.com]

interpretation to actual field data was examined. During the application, both noisy and noiseless anomaly maps were reduced to the pole to determine the horizontal locations of potential structures accurately. Also, the upward continuation process was used in the noisy anomaly map. TA and AGC methods have been applied to both anomaly maps, and the structure boundaries of the model blocks are shown with zero contours (Figures 8 and 9).

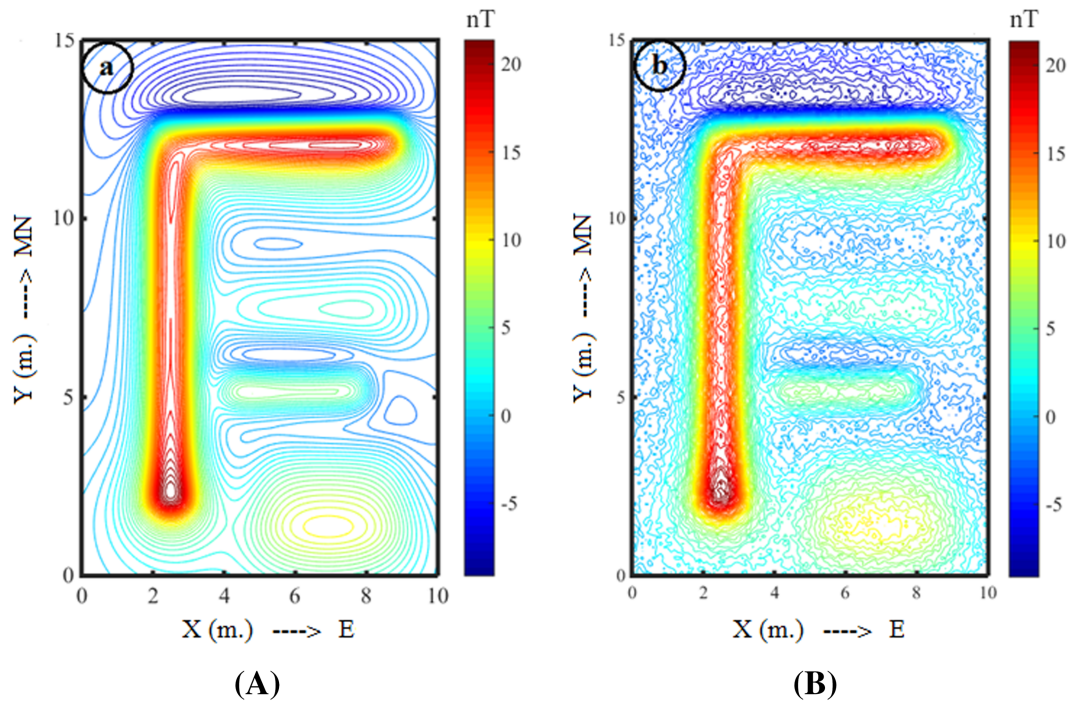


FIGURE 5 Theoretical total magnetic anomaly maps of the synthetic model (inclination angle 60°). (A) Total magnetic anomaly map without noise and (B) total magnetic anomaly map with Gaussian noise [Colour figure can be viewed at wileyonlinelibrary.com]

5 | FIELD APPLICATIONS

Amasya is located between $34^\circ 57' 06''$ (overlined part)– $36^\circ 31' 53''$ East Longitude and $41^\circ 04' 54''$ – $40^\circ 16' 16''$ North Latitude on the Central Black Sea part of the Black Sea Region. Oluz Mound is located in the fertile Plain of Geldingen, which passes through the south of Çekerek River (Zuliya, ancient Skylaks), which is one of the essential branches of Yeşilirmak (ancient Iris) and was discovered during the surveys of Amasya Province between 1997 and 1999.¹⁹ Settled in 3 km south of the Amasya Çorum highway, Oluz Mound lies 2 km northwest of Gözlek Village, approximately 5 km eastern part of Toklucak (Old Oluz) village (Figure 10).

The dimensions of the mound are 280×260 m, and it has the appearance of an almost circle with a size of approximately 130–140 m (Figure 11A). It is approximately 15 m high above the plain level (478.78 m above sea level) and has an area of 45 acres.²⁰ Excavations and geophysical studies have been carried out systematically in the region since 2007. These studies are carried out step by step in line with the plan squares periodically planned by archaeologists (Figure 11B).

5.1 | Magnetometer measurements

In site B, located on the eastern side of Oluz Mound, magnetic measurements were mainly carried out in 2007, 2009, 2010, 2014, and 2015. Littlemore typ 820 proton magnetometer was used for magnetic measurements in geophysical measurements started in 2007. Magnetic measurements were made between site B and site C. Total magnetic field measurements using the proton magnetometer were made in 30×40 m area with 05×05 m profile intervals.

5.2 | Analysis of magnetic data

In order to analyze the magnetic data, the transfer of field data between Surfer and Matlab programs was arranged and converted as input data to the methods suggested during the analysis phase. The total magnetic anomaly map prepared from field measurements used in the interpretation process is given in Figure 12A. Initially, upward continuation and RTP processes were applied to make an accurate numerical analysis of the total magnetic anomaly map of the area in question (Figure 12B,C). The underground structural elements obtained by applying the TA method to the enhanced magnetic anomaly map in Figure 13A are shown in Figure 13B. TA values have the positive values above the causative feature. These values are zero when directly above the source edges. The places where the zero contour passes, determined on

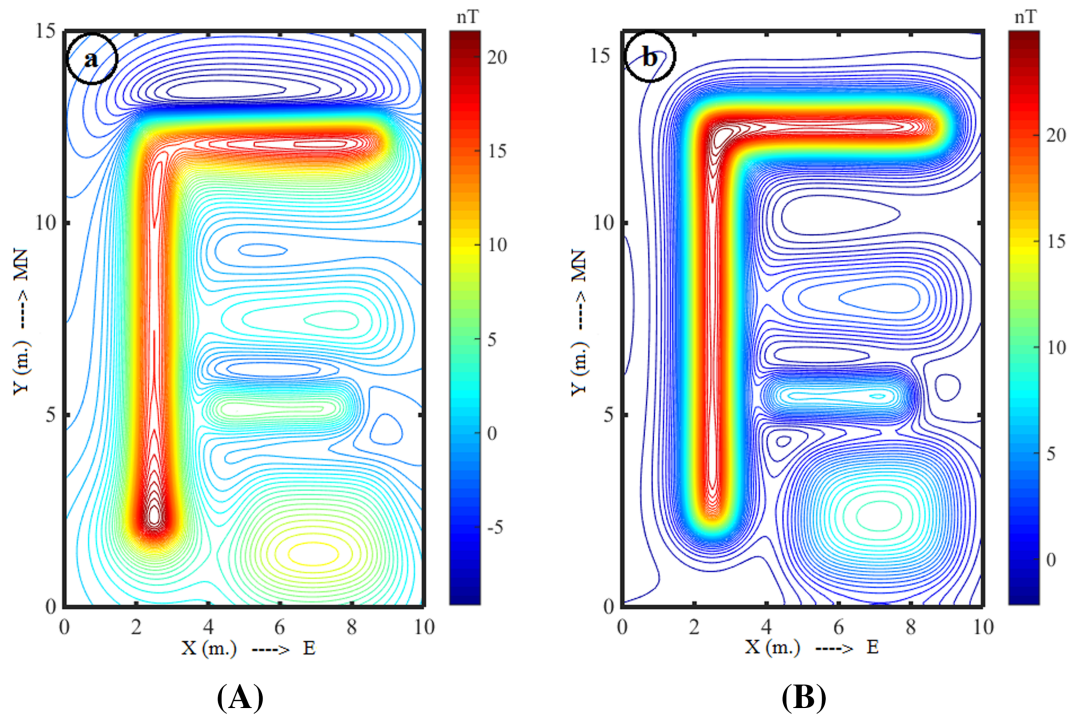


FIGURE 6 (A) Total magnetic anomaly map without noise and (B) reduction to pole map [Colour figure can be viewed at wileyonlinelibrary.com]

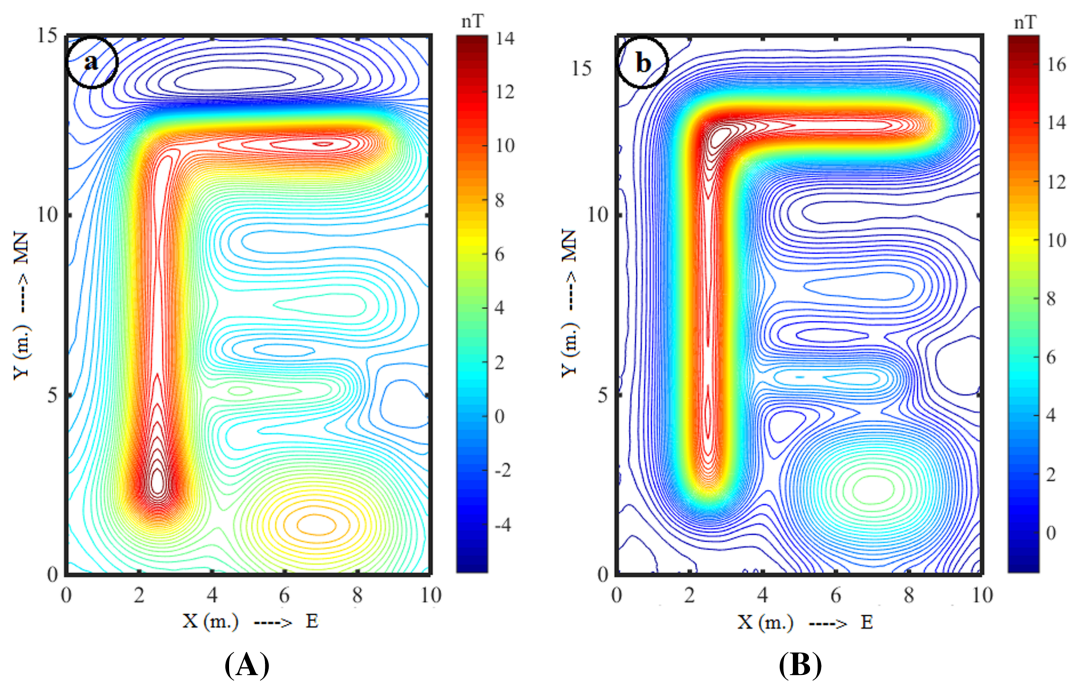


FIGURE 7 (A) Upward continuation map and (B) reduction to pole map [Colour figure can be viewed at wileyonlinelibrary.com]

the map obtained after the TA method is applied, symbolize the edges of archaeological structures belonging to a specific period subsurface, according to the study area. AGC algorithm has been applied to the total magnetic anomaly map given in Figure 13A in order to test the accuracy of the horizontal boundaries obtained by the TA method, and the locations where the zero (0) contours pass are mapped in Figure 13C. It is observed in Figure 13B,C that the horizontal boundaries of the obtained subsurface structure elements show similarities in the results of both methods.

6 | CONCLUSIONS

Numerical analyses of potential structure locations were performed by using derivative-based methods to calculate the horizontal locations of potential subsurface structures that cause anomalies on magnetic anomaly maps. In this context, first, to test the methods considered to be applied in magnetic field data measured in the relevant area, the depths that can be compatible with archaeological subsurface structures are 0.5–1 m. A synthetic model was created consisting of five prismatic blocks. A test model anomaly with an inclination angle of 90° was calculated to test the accuracy of the applied methods with theoretical data with a 60° inclination angle on the designed model. Gaussian noise with a standard

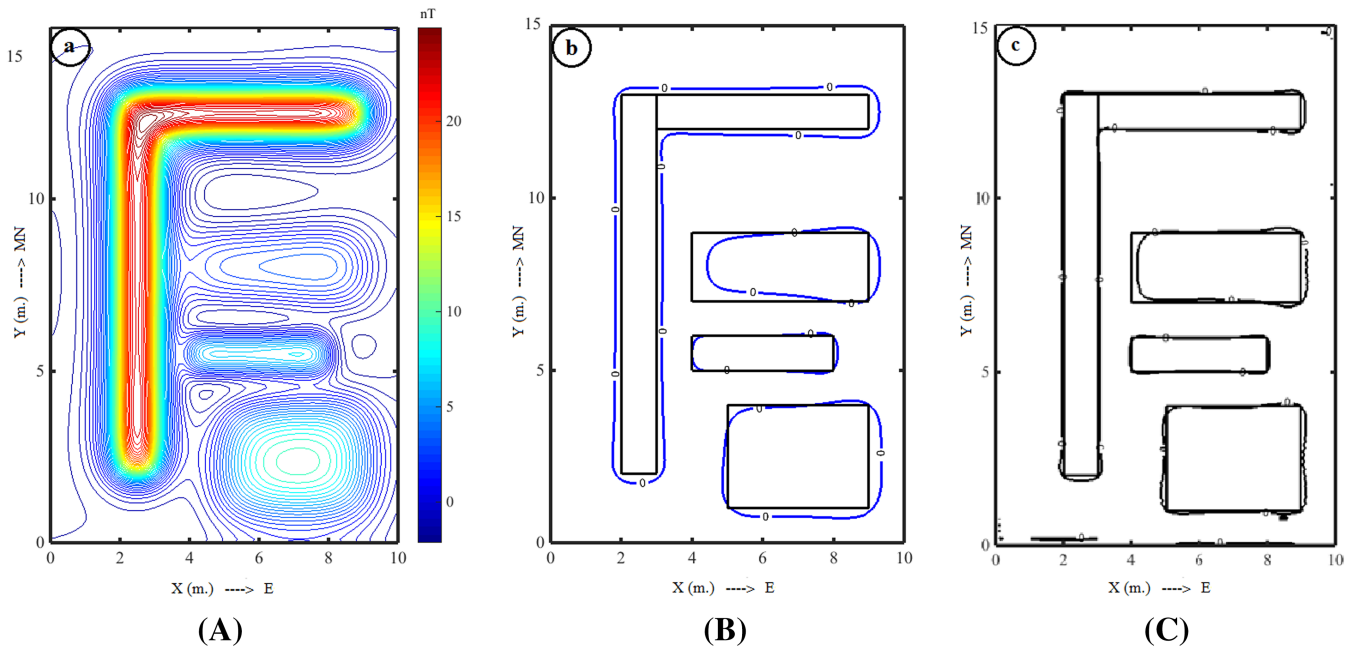


FIGURE 8 (A) Reduction to pole map (belongs to data without noise), (B) tilt angle map (degrees) (model block boundaries are shown in blue), and (C) automatic gain control map [Colour figure can be viewed at wileyonlinelibrary.com]

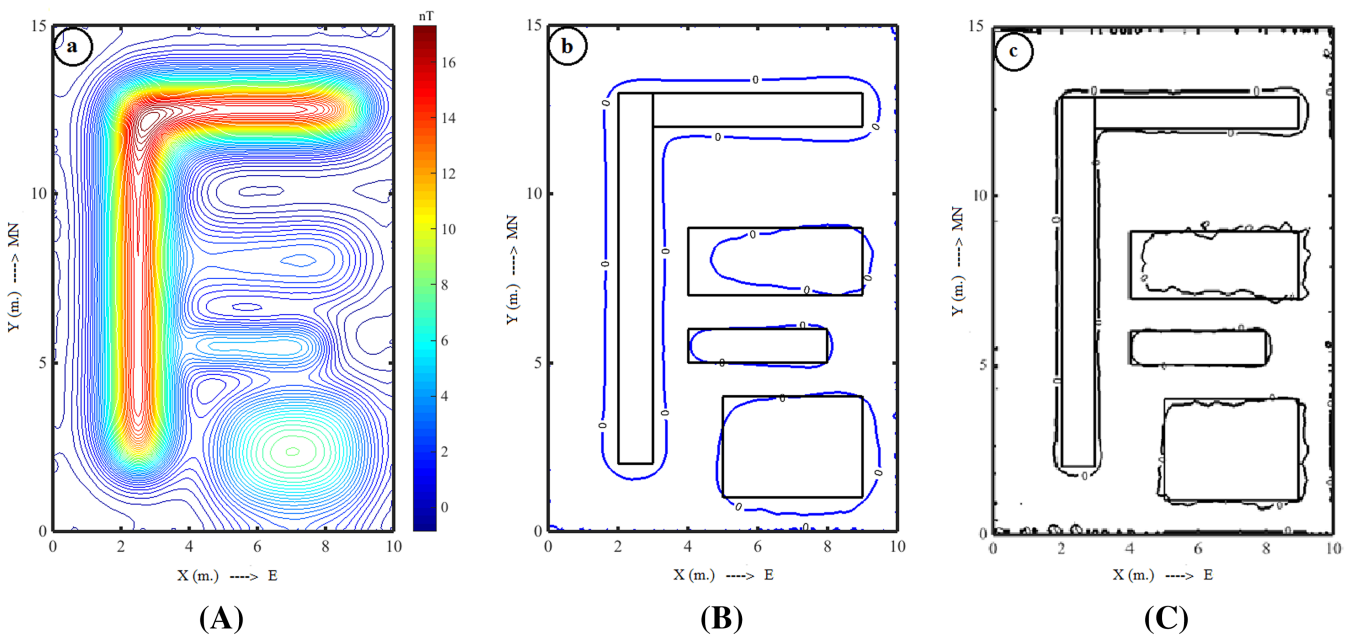


FIGURE 9 (A) Reduction to pole map (belongs to data with noise), (B) tilt angle map (degrees) (model block boundaries are shown in blue), and (C) automatic gain control map [Colour figure can be viewed at wileyonlinelibrary.com]

deviation of 0.3 nT was added to the theoretical data with an inclination angle of 60° to fit the field data. In the data improvement phase, the upward reach method was applied to distinguish regional and residual from the noisy anomaly, and the effect of noise was eliminated. In order to avoid misleading results due to the difference of inclination angle from vertical to the calculated noisy and noiseless data, the theoretical data calculated by applying the RTP method were improved and prepared for interpretation. The applicability of the TA and AGC methods, which are planned to be used to

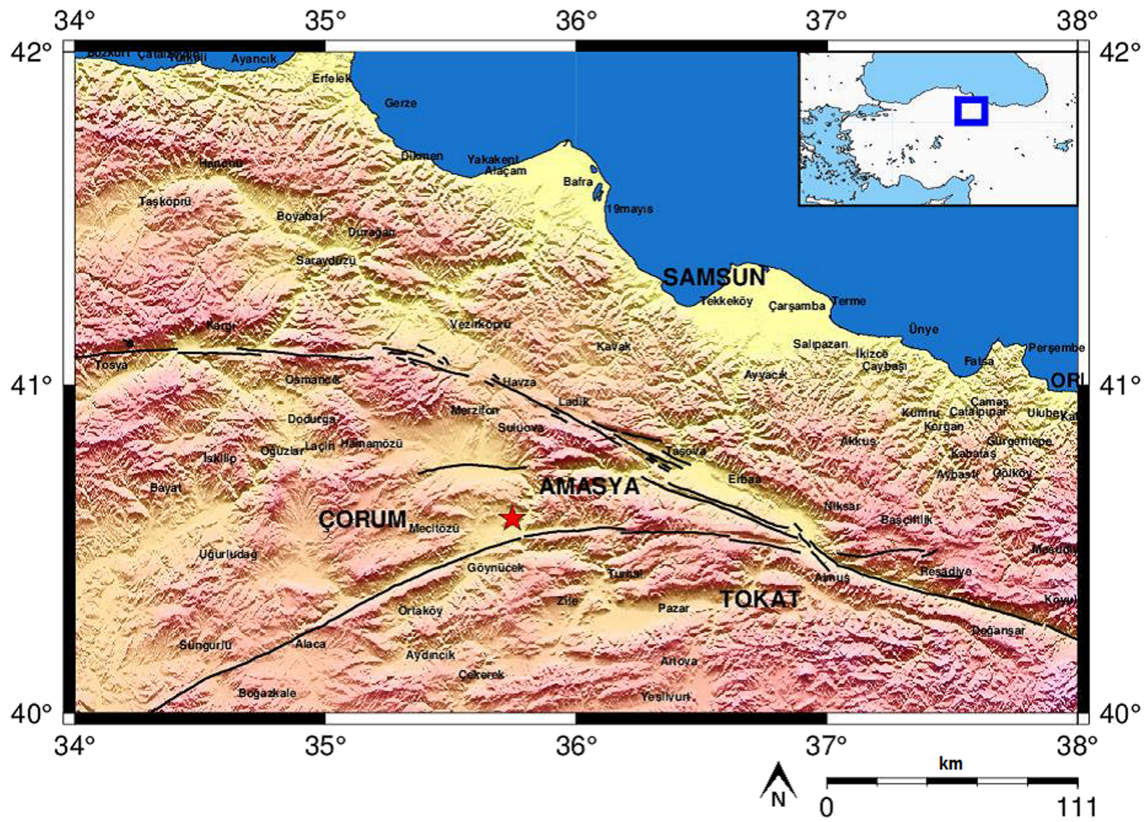


FIGURE 10 Amasya Oluz Mound location map [Colour figure can be viewed at wileyonlinelibrary.com]

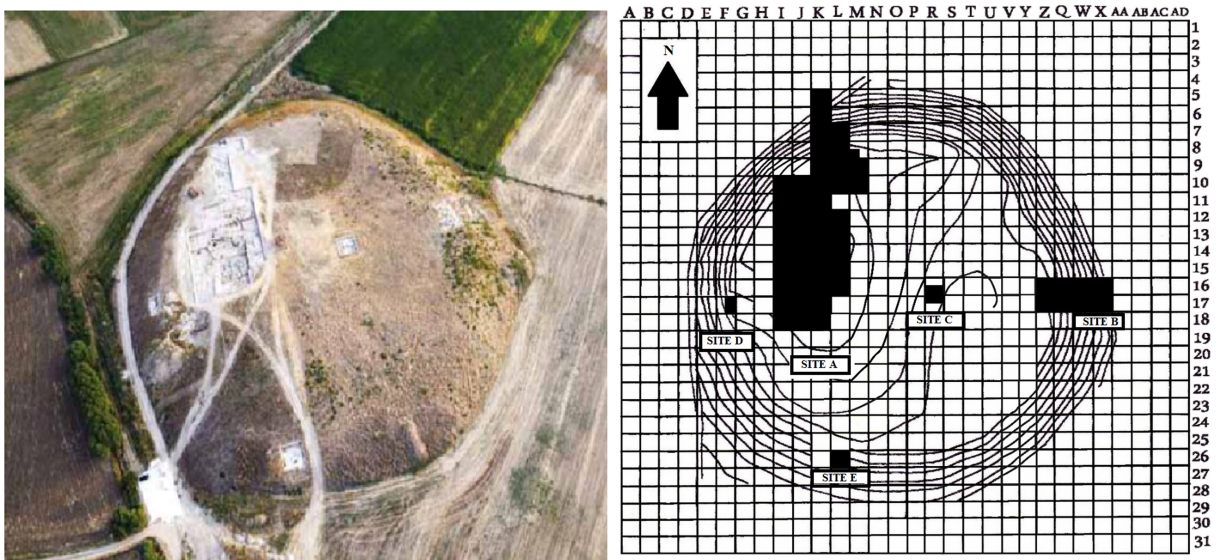


FIGURE 11 (A) Drone view of Amasya Oluz Hoyuk and (B) excavation plan squares²¹ [Colour figure can be viewed at wileyonlinelibrary.com]

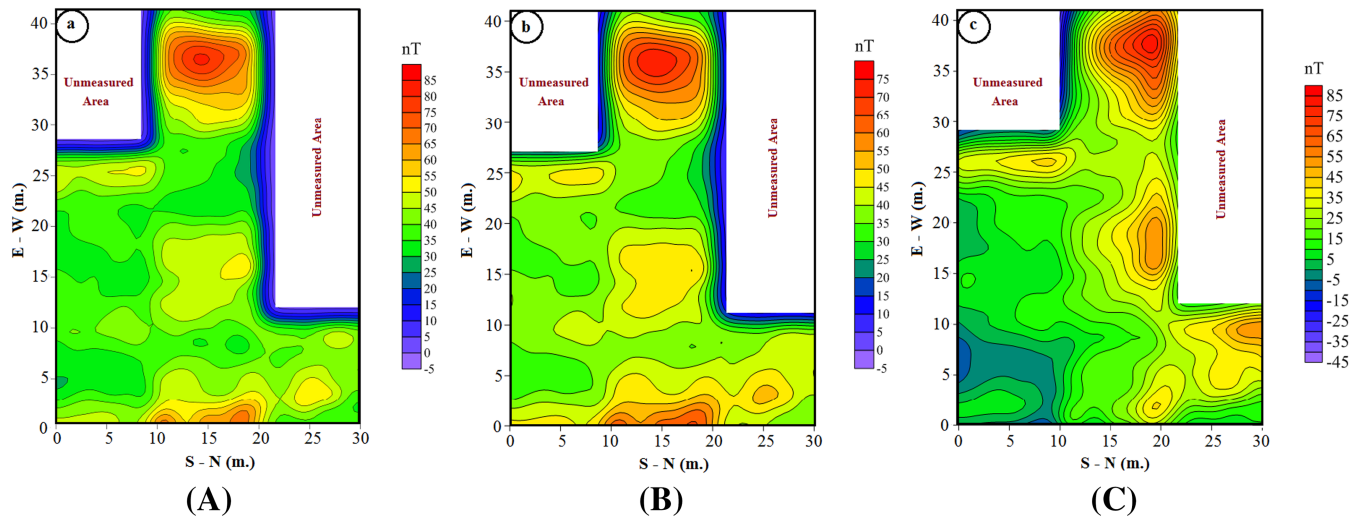


FIGURE 12 (A) Total magnetic anomaly map of the study area (contour interval of 5 nT), (B) upward continuation map (0.3 m), and (C) RTP map [Colour figure can be viewed at wileyonlinelibrary.com]

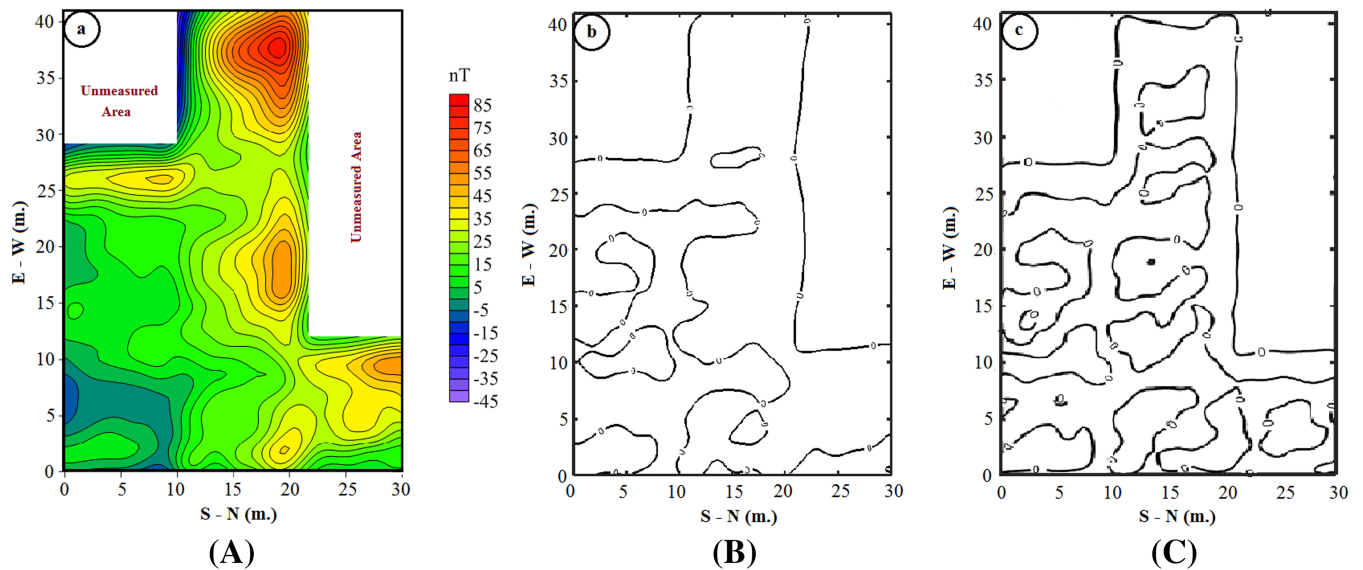


FIGURE 13 (A) RTP map of the study area, (B) tilt angle map, and (C) automatic gain control map [Colour figure can be viewed at wileyonlinelibrary.com]

determine the horizontal boundaries of potential archaeological subsurface structure distributions during the interpretation of the field data, has been tested on noisy and noiseless theoretical data with the programs prepared. The TA method determines the locations of the block structures close to the surface of the model relatively more successfully compared to the building boundaries located deeper. In the presence of noise, it efficiently indicates the building boundaries in realistic positions. By applying the AGC method, which is the most common of the image enhancement techniques, the amplitude distribution in the data is balanced. The structure boundaries are further clarified. Thus, the methods used in determining the horizontal boundaries were tested. The total magnetic field measurements using the proton magnetometer in the Amasya Oluz Mound archaeological excavation area were made at the corners of the grid at 0.5×0.5 m intervals in an area of 30×40 m. The map was created with the magnetic data obtained. The data prepared with the Surfer program were transferred to the Matlab environment using a converter program prepared in the Matlab environment. Noise effects were eliminated from the field data by applying the upward continuation method, used as a data improvement method, to the total magnetic field anomaly obtained (0.3 m). To determine the horizontal boundaries, the

locations of potential subsurface archaeological structure distributions that cause anomaly have been revealed by applying the TA and AGC methods to the field data. Architectural building foundations that form a corner in the region and road routes between these structures were visualized. Since these routes may be covered with architectural stone debris, they cannot give complete linearity. Using these methods, the horizontal position parameters of the potential historical settlement were analyzed. A preliminary study was carried out to shed light on the planning of the archaeological excavations, which are planned to be carried out to uncover the historical heritage in the relevant area by obtaining maps of potential subsurface archaeological structures by using the calculated geometric parameters. As a continuation of this study, which will be the second part of quantitative analysis of total magnetic anomaly maps on archaeological sites, it is planned to complete the quantitative analysis of the total magnetic anomaly map of the region by calculating the depth values of the potential buried structures found in the excavation area.

ACKNOWLEDGEMENT

The authors would like to express their gratitude to Şevket Dönmez and the excavation crew for enabling us to apply geophysical methods in the excavation site.

CONFLICT OF INTEREST

The authors declare no potential conflict of interests.

ORCID

Hazel Deniz Toktay  <https://orcid.org/0000-0002-3806-489X>

Davut Aydoğan  <https://orcid.org/0000-0001-8792-2099>

Fethi Ahmet Yüksel  <https://orcid.org/0000-0003-2207-1902>

REFERENCES

1. Drahor MG. Arkeolojik Alanların Özdirenc Ve Dogal Gerilim (SP) Yontemleri ile Arastırılması (in Turkish). Ph D Dissertation 1993;14(3):210.
2. Evjen HM. The place of the vertical gradient in gravitational interpretations. *Geophysics*. 1936;1(1):127-136.
3. Miller H, Singh V. Potential field tilt - a new concept for location of potential field sources. *J Appl Geophys M*. 1994;32(2):213-217.
4. Wjns C, Perez C, Kowalczyk P. Theta map: Edge detection in magnetic data. *Geophysics*. 2005;70(4):39-43.
5. Cooper GRJ, Cowan DR. Enhancing potential field data using filters based on the local phase. *Comput Geosci*. 2006;32(10):1585-1591.
6. Salem A, Williams S, Fairhead JD, Ravat D, Smith R. Tilt-depth method: A simple depth estimation method using first-order magnetic derivatives. *Lead Edge*. 2007;26(12):1502-1505.
7. Verduzco B, Fairhead JD, Green CM, MacKenzie C. New insights into magnetic derivatives for structural mapping. *Lead Edge*. 2004;23(2):116-119.
8. Ma G, Li L. Edge Detection in Potential Fields with the Normalized Total Horizontal Derivative. *Comput Geosci*. 2012;41:83-87.
9. Blakely RJ. *Potential Theory in Gravity and Magnetic Applications*. London: Cambridge University Press; 1995.
10. Henderson RG, Zietz I. The Upward Continuation of Anomalies in Total Magnetic Intensity Fields. *Geophysics*. 1949;14(4):517-534.
11. Foss C. *Magnetic Data Enhancements and Depth Estimation:736-746*. Dordrecht: Springer Netherlands; 2011.
12. Luo Y, Xue DJ, Wang M. Reduction to the pole at the geomagnetic equator. *Chin J Geophys*. 2010;53(6):1082-1089.
13. Milligan P, Gunn P. Enhancement and presentation of airborne geophysical data. *AGSO J Austr Geol Geophys*. 1997;17(2):63-75.
14. Baranov V, Naudy H. Numerical calculation of the formula of reduction to pole. *Geophysics*. 1964;29(1):67-79.
15. Oruc B, Selim H. Interpretation of magnetic data in the Sinop area of Mid Black Sea, Turkey, using tilt derivative, Euler deconvolution, and discrete wavelet transform. *J Appl Geophys*. 2011;74(4):194-204.
16. Rajagopalan S, Milligan P. Image enhancement of aeromagnetic data using Automatic Gain Control. *Exp Geophys*. 1994;25(4):173-178.
17. Cooper GRJ. The automatic interpretation of geophysical data. In: Seventh SAGA Biennial Technical Meeting and Exhibition; 2001; South Africa.
18. Rajagopalan S. IThe use of 'Automatic Gain Control' to display vertical magnetic gradient data. *Exp Geophys*. 1987;18(1-2):166-169.
19. Yüksel FA. Amasya Oluz Höyük 2009-2012 Yılları Arası Arkeojeofizik Çalışmaları:363-397. Amasya: Amasya Valiliği 2017.
20. Dönmez Ş. *Oluz Höyük Kazı Sonuçları Serisi 2 Amasya - Oluz Höyük Kuzey - Orta Anadolu'da Bir Akhaimenid (Pers) Yerleşmesi,2009-2013 Dönemi Çalışmaları Genel Değerlendirmeler Ve Önsonuçlar (in Turkish)*. Amasya: Bizim Ofset Press; 2017.
21. Dönmez Ş, Beyazıt AY, Kaymakçı A, Adısönmez B, Abazoğlu F. Oluz Höyük Kazısı Dokuzuncu Dönem Çalışmaları 2007 Yılı Jeofizik Uygulamaları (in Turkish). In: 38. Kazı Sonuçları Toplantısı; 537-552; Edirne.

How to cite this article: Deniz Toktay H, Aydoğan D, Yüksel FA. Quantitative analysis of total magnetic anomaly maps on archaeological sites—Part 1. *Math Meth Appl Sci*. 2021;1-15. <https://doi.org/10.1002/mma.7652>